Energy 173 (2019) 721–731

Contents lists available at ScienceDirect

Energy

journal homepage: www.elsevier.com/locate/energy

Simultaneous experimental comparison of low-GWP refrigerants as drop-in replacements to R245fa for Organic Rankine cycle application: R1234ze(Z), R1233zd(E), and R1336mzz(E)

Jingye Yang [a], Zhenhong Ye [a], Binbin Yu [a], Hongsheng Ouyang [b], Jiangping Chen [a, *]

[a] *Institute of Refrigeration and Cryogenics, Shanghai Jiao Tong University, Shanghai, 200240, PR China*
[b] *State Key Lab for Fluorine Greenhouse Gases Replacement and Control Treatment, Zhejiang Research Institute of Chemical Industry, Hangzhou, PR China*

A R T I C L E I N F O

Article history:
Received 14 September 2018
Received in revised form
8 January 2019
Accepted 7 February 2019
Available online 18 February 2019

Keywords:
Organic rankine cycle
Alternatives
Low GWP
R1234ze(Z)
R1233zd(E)
R1336mzz(E)

A B S T R A C T

Micro-scale organic Rankine cycle (ORC) enables to convert low-temperature waste heat into electricity, which is presented as one of combined heat and power (CHP) technologies. The commonly utilized working fluid R245fa will be phased out in the near future because of significant impact to the climate change. In that case, new HFOs (hydrofluoroolefins) refrigerants are suggested as potential alternatives to R245fa because of extremely low GWPs (Global Warming Potential) and zero ODP (Ozone Depletion Potential). This paper experimentally analyzed the applicability of three HFO refrigerants as drop-in replacements to R245fa for micro-scale ORC application including R1234ze(Z), R1233zd(E) and R1336mzz(E). Control options were assigned to the refrigerant mass flow rate and the expander rotational speed. System performance indicators including cycle thermal efficiency and net power output were compared. Besides, the expansion behavior along with the heat transfer performance and pump work were also analyzed. For the whole range of operating conditions, comparing the maximum cycle thermal efficiency, R245fa is 4.6% while R1233zd(E), R1234ze(Z) and R1336mzz(E) are 4.7%, 4.5% and 3.1%, respectively; Comparing the maximum net power output, R245fa generates 11.4% more than R1233zd(E) and 3.1% than R1234ze(Z). Limited range of pressure ratio contributes to the extremely low electricity of R1336mzz(E).

1. Introduction

Escalating consumption of fossil fuels and emissions of greenhouse gases have raised the great concern about the sustainable environment development recently. The efficient utilization of global supply energy becomes a major challenge nowadays. Organic Rankine cycle is presented as one of viable combined heat and power technologies to meet the aforementioned requirements. In terms of low-grade heat sources, refrigerants are commonly utilized as working fluids to recover the wasted energy. R245fa has been considered as the most appropriate working fluid for low temperature heat source in previous literature. However, the relatively high GWP (Global Warming Potential) of R245fa has significant impact to climate change, which is suggested to be phased out in the near future. In 1997, HFCs (Hydrofluorocarbons) were considered as GHG (Green House Gas) according to Kyoto Protocol [1]. European Parliament [2] suggested to ban the HFCs with a GWP higher than 150 in domestic refrigerators by 2015. The Kigali amendment [3] was approved in the 28th conference of the parties to the Montreal Protocol. The historic limitation of green-house gas HFCs was realized (Montreal-Protocol, 2016).

Screening criteria of selecting appropriate alternatives to R245fa for organic Rankine cycle application includes the thermodynamic properties, global safety evaluation such as non-toxicity and environmental impact indicator (e.g. ODP, GWP). Recently, new HFO refrigerants are suggested as substitutes to R245fa with great potential because of similar thermodynamic properties. What is more, the extremely low GWPs and zero ODP of new refrigerants show the privileges to HFCs.

Several simulations have been concentrated on the aforementioned new type working fluids based on the organic Rankine cycle system. Noboru Yamada et al. [4] proposed a fundamental thermodynamic model of five types of ORC to evaluate the thermal efficiency of R1234yf compared to R134a. He concluded that

* Corresponding author.
E-mail address: [redacted]@163.com (J. Chen).

https://doi.org/10.1016/j.energy.2019.02.054
0360-5442/

R1234yf is a potential working fluid for recovery of low-to-medium temperature heat source. Dong Luo et al. [5] created a systematic model of basic organic Rankine cycle to evaluate the performance using both pure working fluids and mixtures. Multiple heat source temperatures were involved to investigate the performance of candidates with low-GWPs for further design evaluation. Wei Liu et al. [6] studied eight HFO refrigerants with low-GWPs for ORC application in geothermal power generation area. A standard ORC simulation was conducted. Heat transfer efficiency along with the thermal efficiency were considered as main criterion to evaluate the system performance. Results indicated that some of HFO refrigerants show promising performance especially for low-to-medium temperature geothermal ORC application. Philipp Petr et al. [7] provided a comparative theoretical analysis of R1234ze(Z) and R245fa in organic Rankine cycle. Heat source temperature varied from 100 °C to 250 °C in system simulation. The results reflected that R1234ze(Z) is an appropriate drop-in replacement to R245fa, though noticeable performance losses were observed for heat source temperature range between 183 °C and 224 °C. Davide Ziviani et al. [8] developed a dedicated steady-state model of micro-scale regenerative ORC, which is applied to evaluated the applicability of R1234ze(Z) as an alternative to R245fa. The heat source temperature ranges from 90 °C to 120 °C, which is simulated by a thermal oil heater. Muhammad Usman et al. [9] provided a thermo-economic comparison between R1233zd(E) and R245fa based on a mathematical model of geothermal organic Rankine cycle. The results revealed that R1233zd(E) has potential to replace R245fa if the heat source temperature is higher (e.g. 145 °C). Francisco Moles et al. [10] theoretically compared three working fluids both in basic ORC and regenerative ORC. The results showed that R1233zd(E) leads to higher net cycle efficiency than R245fa and consumes lower pump power. An additional recuperator is benefit to improve the performance of R1336mzz(Z).

Apart from the numerical simulations concerning possible alternatives, there are also some experimental investigations in previous literature. Ryuichi Nagata et al. [11] comparatively assessed the convective condensation and pool boiling heat transfer coefficients of three low-GWP refrigerants including R1234ze(E), R1233zd(E) and R1234ze(Z) on a horizontal smooth tube made of copper. Joaquín Navarro-Esbrí et al. [12] experimentally conducted an evaluation of R1336mzz(Z) as a drop-in replacement to R245fa for low-temperature micro-scale ORC application. The results indicated that R1336mzz(Z) leads to higher net electrical efficiency, isentropic expander efficiency and volumetric expander performance than R245fa in the same experimental equipment. Ludovic Guillaume et al. [13] conducted comparative experimental tests between two different working fluids including R245fa and R1233zd(E) in ORC system, which is integrated with an oil-free radial-inflow turbine. In order to identify the most suitable working fluid, three comparison methods were applied to the research. Sebastian Eyerer et al. [14] implemented a comparative experimental investigation between R1233zd(E) and R245fa. The influences of the process parameters such as mass flow rate and expander rotational speed on system performance were analyzed. The results showed that R1233zd(E) leads to 6.92% higher thermal efficiency than R245fa while generates lower electrical power.

Remarkable contributions have been made to prove the applicability of new HFO refrigerants as working fluids in organic Rankine cycle system in published works. However, limited experimental studies of different low-GWP refrigerants were conducted considering the availability of various HFO refrigerants on commercial markets. Moreover, simultaneous experimental comparison among multiple potential alternatives haven't been implemented in previous researches. In this paper, three latest new low-GWP refrigerants including R1233zd(E), R1234ze(Z), R1336mzz(E) are experimentally investigated in ORC system as drop-in replacements to R245fa. Among them, R1234ze(Z) and R1336mzz(E) were first-time experimentally tested, which can be valuable reference to other researchers. The influence of the process parameters on system performance are studied under the heat source temperature around 125 °C. To better summarize the overview researches and demonstrate the soundness of current research, Table 1 shows the list of published works about the state of the art.

The remainder of this paper is processed with four sections: first section compared the basic thermo-physical properties of three working fluids. Primary thermodynamic analysis was implemented to give a prior provident of the applicability of new refrigerants in micro-scale ORC system; In the second section, an experimental test rig was designed and optimized for R245fa as a baseline, the rest of refrigerants were experimentally tested as drop-in replacements to R245fa in the same test bench; In the third section, the system performance along with the expansion behavior, heat transfer procedure and pump energy consumption were compared; Several conclusions were drawn based on the experimental results in the final section.

Table 1
State of the art.

Simulation	
Related work	Key innovations
Noboru Yamada et al., [4]	Presented the thermodynamic model of five types of ORC to evaluate the thermal efficiency of R1234yf compared to R134a
Dong Luo [5]	Both pure fluids and mixtures were studied. Multiple heat sources were involved.
Wei Liu [6]	Eight low-GWP HFO refrigerants were investigated in geothermal power generation area
Philipp Petr et al., [7] Davide Ziviani et al., [8]	Theoretical analysis of R1234ze(Z) as alternative to R245fa for ORC application. Heat source temperatures were varied to different values
Muhammad Usman et al., [9]	A thermo-economic comparison between R1233zd(E) and R245fa
Francisco Moles et al., [10]	Theoretical analysis among three refrigerants including R1233zd(E), R1336mzz(Z) and R245fa based on the basic ORC and regenerative ORC.
Experimental investigation	
Ryuichi Nagata et al., [11]	Experimentally investigated the heat transfer coefficients of three different refrigerants (e.g. R1234ze(E), R1233zd(E) and R1234ze(Z)) on a horizontal smooth tube.
Joaquín Navarro-Esbrí et al., [12]	Experimentally compared R1336mzz(Z) to R245fa
Ludovic Guillaume et al., [13] Sebastian Eyerer et al., [14]	Experimentally compared R1233zd(E) and R245fa
This work Experimental research	Simultaneous experimental investigation among four refrigerants (e.g. R245fa R1233zd(E) R1234ze(Z) and R1336mzz(E)) R1234ze(Z) and R1336mzz(E) were first-time experimental tested

Table 2
Comparison of thermo-physical properties between refrigerants.

Parameter	R245fa	R1233zd(E)	R1234ze(Z)	R1336mzz(E)
Formula	$C_3H_3F_5$	$C_3ClH_2F_3$	$C_3H_2F_4$	$C_4H_2F_6$
Molecular mass [kg/mol]	134.03	130.5	114.04	164.05
Critical temperature [°C]	154.01	165.6	153.7	137.7
Critical pressure [bar]	36.5	35.7	35.3	31.5
Normal boiling point [°C]	14.81	17.92	9.7	7.5
Slope ds/dT	Positive	Positive	Isentropic	Positive
ODP	0	0.00034	0	0
GWP	858	1	<1	7
ALT	7.7	0.07	0.027–0.049	n.a.
ASHARE safety classification	B1	A1	A2L	A1
Flammability	Non-flammable	Non-flammable	7.5–16.4 vol%	Non-flammable
Toxicity	Non-toxic	Non-toxic	Non-toxic	n.a.

2. Comparison of ORC working fluids properties

2.1. Thermo-physical properties

Screening criteria of possible replacements for R245fa concerning three factors. First of all, the substitutes should exhibit the similar thermodynamic properties with R245fa; secondly, the working fluids should meet the global safety standards including non-toxicity, non-flammable and non-corrosion; last but not the least, the substitutes are preferred to be with zero ODP and extremely low GWP. This section compares the thermo-physical properties among four refrigerants, as summarized in Table 2.

Apart from the basic thermo-physical properties, initial cost should be taken into consideration as well. The initial cost consists of two main parts including the material cost and the carbon tax. The fact is that three new HFO refrigerants haven't been available on worldwide commercial market yet and no official price can be taken as reference. Refrigerants tested in current research were samples from supportive laboratory. In that case, only a primary cost estimation based on the normalized ingredient was implemented in this section as reference for researchers. For example, the material cost of R1234ze(Z) is assumed to be 1.7–1.9 times of R245fa based on the manufacturing cost according to the supportive laboratory for current research. Carbon tax is charged 25 dollars for per kg of CO2 according to the European union F-gas legislation [15]. Carbon tax of three new HFO refrigerants can be exempt based on the F-gas legislation. On account of that, the initial cost of the alternative is capable to supersedes carbon tax of R245fa. Another example is that purchase cost of R245fa mentioned in Eyerer published work [14] was about 30–35 €/kg while for the new generation refrigerant R1233zd(E) was between 20 and 25 €/kg. Thus, the price of R1233zd(E) is considered competitive to R245fa as drop-in replacement. However, the cost is involved with the purchase quantity and the distribution channels.

2.2. Thermodynamic analysis

In order to predict the applicability of the new HFO refrigerants as drop-in replacements to R245fa for ORC utilization, a preliminary thermodynamic analysis was conducted in this section. The thermodynamic analysis is a fundamental link of substitute investigation that gives a prior prediction of new refrigerants including R1233zd(E), R1234ze(Z) R1336mzz(E) as applicable alternatives to R245fa. Furthermore, the thermodynamic analysis among four refrigerants was also prepared for the lateral experimental tests. Additionally, the basic equations for cycle performance calculation were presented in this section.

Fig. 1 presents the configuration of basic organic Rankine cycle (BORC) with four main equipment. Fig. 2 describes the T-s diagram

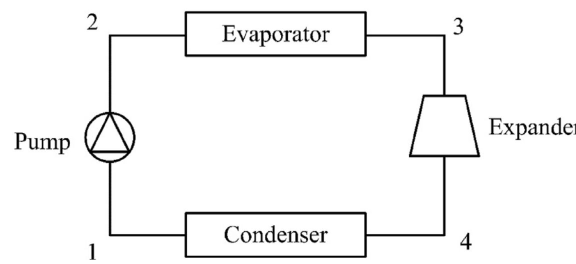

Fig. 1. Basic organic Rankine cycle.

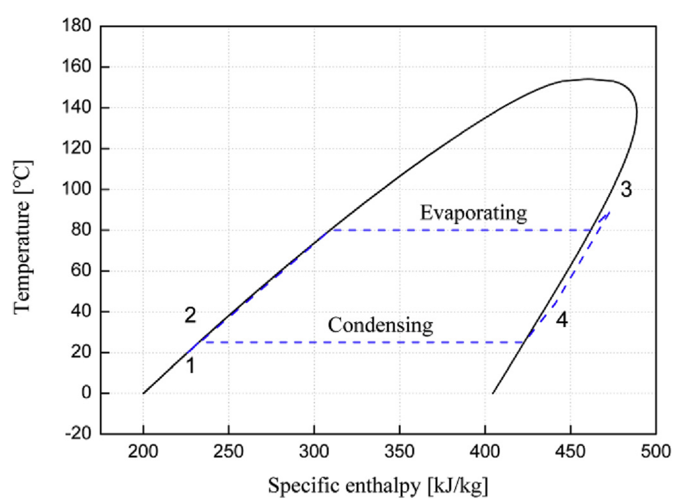

Fig. 2. T-*h* diagram of basic ORC.

of ORC accordingly. The principle can be described as follows: first of all, the working fluid is pumped into the evaporator to absorb the heat from the heat source; afterwards, the superheated vapor expands inside the expander to generate electricity with a coupled generator; subsequently, the exhaust vapor is cooled by the cooling water; eventually, the subcooled fluid is pumped back in to the liquid pump to complete the whole cycle. Basic equations are summarized in Table 3, which are used to model each configuration.where $\dot{W}_p$ and $\dot{W}_x$ represent the pump power and expansion work; $\eta_{p,is}$ and $\eta_{p,em}$ are referred to the pump isentropic efficiency and pump electromechanical efficiency; $\dot{M}_{ref}$ is refrigerant mass flow rate; h_{in} and h_{out} represent the specific enthalpy at the inlet and outlet of each configuration; $\dot{Q}_{ev}$ and $\dot{Q}_{cd}$ are referred to the heat transfer rate in the evaporator and condenser. $\eta_{x,is}$ and η_{vol} are expander isentropic efficiency and volumetric efficiency,

Table 3
Basic equations for each configuration.

Component	Characteristic equations
pump	$\eta_{p,is} = \frac{h_{out,is} - h_{in}}{h_{out} - h_{in}} \dot{W}_p = \dot{M}_{ref}(h_{p,in} - h_{p,out})/\eta_{p,em}$
Evaporator	$\dot{Q}_{ev} = \dot{M}_{ref}(h_{ev,out} - h_{ev,in})$
Condenser	$\dot{Q}_{cd} = \dot{M}_r(h_{cd,in} - h_{cd,out})$
Expander	$\eta_{x,is} = \frac{h_{x,in} - h_{x,out}}{h_{x,in} - h_{x,out,is}} \dot{W}_x = \eta_{x,em}\eta_{vol}\dot{M}_{ref}(h_{x,in} - h_{x,out})$
Cycle	$\eta_{cycle} = (\dot{W}_x - \dot{W}_p)/\dot{Q}_{ev}$

respectively. Thermodynamic properties of refrigerants are obtained from the Equation of state (EOS) based software REFPROP.NIST [16].

For organic Rankine cycle system, cycle thermal efficiency is a comprehensive performance indicator that involves with output electricity, pump energy consumption and heat transfer rate in evaporator, which is frequently used to evaluate the system performance. In this section, the operational parameters are assigned to the evaporating temperature, condensing temperature and the superheating with a given heat rate transferred into evaporator 10 kW. In each analysis, one of the operational parameters is varied according to Table 4 while the rest of them are maintained as constants. Efficiencies are assumed as constants in thermodynamic analysis. The impacts of aforementioned parameters on the cycle thermal efficiency are analyzed. Literally, concerning the thermodynamic analysis, no pressure drops, heat losses and other factors affecting the actual system performance are assumed.

In the first analysis, evaporating temperature is varied according to Table 4 while maintaining the condensing temperature at 25 °C and superheating at 5 °C. Fig. 3 shows the evolution of cycle thermal efficiency to various evaporating temperatures. For all the refrigerants, the cycle thermal efficiency increases with the evaporating temperature. This can be explained with the theoretical T-*h* diagram of the basic ORC, as shown in Fig. 2. The increasing evaporating temperature is resulted from higher evaporating pressure, which contributes to the higher suction pressure of the expander. When the condensing temperature is maintained as the same, the potential expansion power increases with the evaporating temperature. Thus, the cycle thermal efficiency will increase with evaporating temperature under the fixed input heat rate. R1233zd(E) and R1234ze(Z) show similar performance and both of them lead to higher cycle thermal efficiency than R245fa, which can be explained with higher saturation temperature. For the same given operating pressure, both of them can achieve higher evaporating temperature than R245fa, which is beneficial for cycle thermal efficiency.

Table 4
Operating conditions.

Parameters	Numerical value
Evaporating temperature [°C]	80,90,100,110,120,130
Condensing temperature [°C]	25,30,35,40,45
Superheating [°C]	5,10,15,20,25
Subcooling [°C]	5
Efficiencies [$\eta_{x,is}$ η_{vol}, $\eta_{p,is}$]	0.85
Efficiencies [$\eta_{x,em}$]	0.95
Efficiencies [$\eta_{p,em}$]	0.45

In the second analysis, condensing temperature is varied according to Table 4 while maintaining the evaporating temperature at 110 °C and superheating at 5 °C. The increasing condensing temperature has negative impact on the cycle thermal efficiency, as shown in Fig. 4. This can be understood in the same manner as Fig. 3. The increasing condensing temperature is resulted from higher exhaust pressure of the expander, in that case, the potential expansion power on expander side will decrease. Thus, the cycle thermal efficiency will decrease with higher condensing temperature.

In the third analysis, superheating is varied according to Table 3 while maintaining the evaporating temperature at 110 °C and condensing temperature at 25 °C. Fig. 5 indicates the influence of superheating on the system performance. Obviously, different refrigerants show various behavior according to Fig. 5. This mainly because of the classification of working fluids in organic Rankine cycle. Both R245fa and R1233zd(E) belong to the dry working fluid with positive saturation vapor slope. R1234ze(Z) is categorized as isentropic working fluid, in this case, appropriate superheating at the expander inlet is necessary to avoid the liquid entering into two-phase region at the end of the expansion procedure.

Literally, in thermodynamic analysis, no pressure drops, heat losses and other factors affecting the actual system performance are considered. Practical performance with various component designs and operating conditions may not be accurately predicted because of nonlinear behaviors. In that case, the parametric behavior of the system in practical experiments can be quite

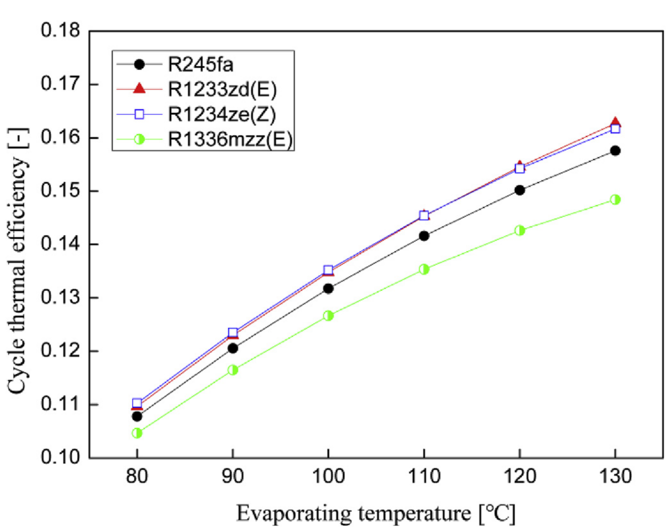

Fig. 3. Evolution of cycle thermal efficiency to evaporating temperature.

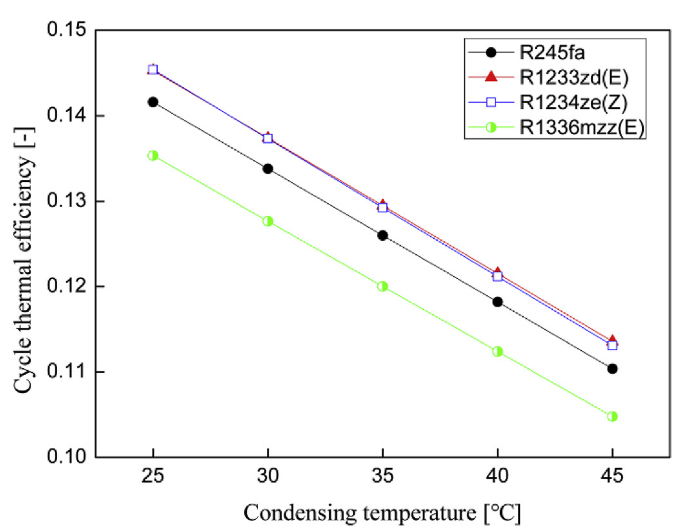

Fig. 4. Evolution of cycle thermal efficiency to condensing temperature.

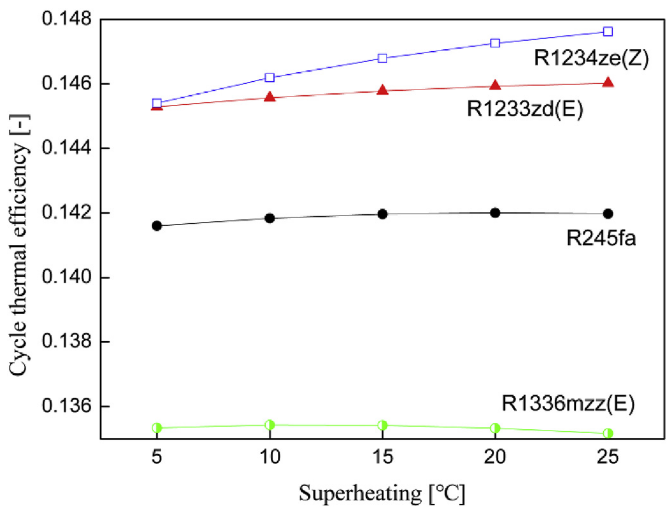

Fig. 5. Evolution of cycle thermal efficiency to superheating.

different. The distinctions between the ideal thermodynamic comparison and experimental performance will be presented in the lateral section. Three low-GWP refrigerants showed very similar performance to R245fa based on the theoretical thermodynamic analysis. Experimental investigation is demanded to further discuss the applicability of aforementioned substitutes in ORC system.

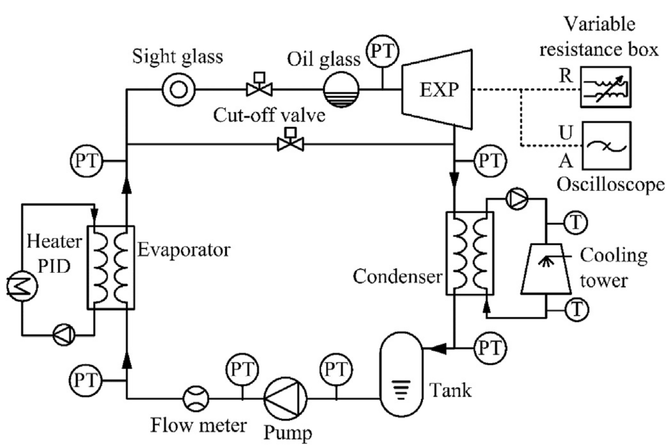

Fig. 6. Conceptual schematic of ORC test rig.

3. Experimental apparatus and methodology

3.1. ORC test rig

Fig. 6 shows the conceptual schematic of the single-pressure organic Rankine cycle system. The test bench consists of three loops including the thermal oil heating loop, cooling water loop and the basic organic Rankine cycle. The heat source temperature is imitated by the thermal oil heater with a PID controller. The maximum temperature of the thermal oil can be achieved around 300 °C. The water of the cooling loop is fed with the outside cooling water tower. The standard organic Rankine cycle consists of four main components including the liquid pump, the evaporator, the expander and the condenser. The operating principle has already been described in section 2.

Fig. 7 summarizes the system components that construct the organic Rankine cycle. Fig. 7a shows a plunger diagram pump used in current system, which is capable to achieve high pressure with small mass flow rate. A motor feature with 1.1 kW 3-phase 380 V is magnetically coupled to this pump. The mass flow rate can be adjusted to different values using the variable pump stroke. The maximum pressure can be achieved around 3000 kPa by this liquid pump. The grazed plate type heat exchangers are utilized as both evaporator and condenser for heat transfer procedures, as shown in Fig. 7b. Thermal insulation cotton was used to rap the whole evaporator to reduce the heat dissipation loss to the ambient environment. Fig. 7c shows a hermetic scroll expander that is modified from a commercial compressor with the swept volume around 50 cm^3. The built-in volume ratio of the volumetric expansion machine is 2.2. Scroll expander has compact structure with less moving parts and lower level of noise [17,18], which is suitable for small scale cogeneration system application. In terms of the hermetic type, the generator is integrated inside the scroll expander shell and the rotary speed range is between 1000 and 3600 rpm. Compared to the open-drive type, the hermetic scroll expander consumes less mechanical friction loss. Moreover, the coupled generator leads to higher electrical efficiency. The expander rotational speed is varied by the Resistance box. An oscilloscope is used to record the voltage and electric current for counter calculation of rotary speed. Apart from the main components, some auxiliary equipment are also utilized to ensure the

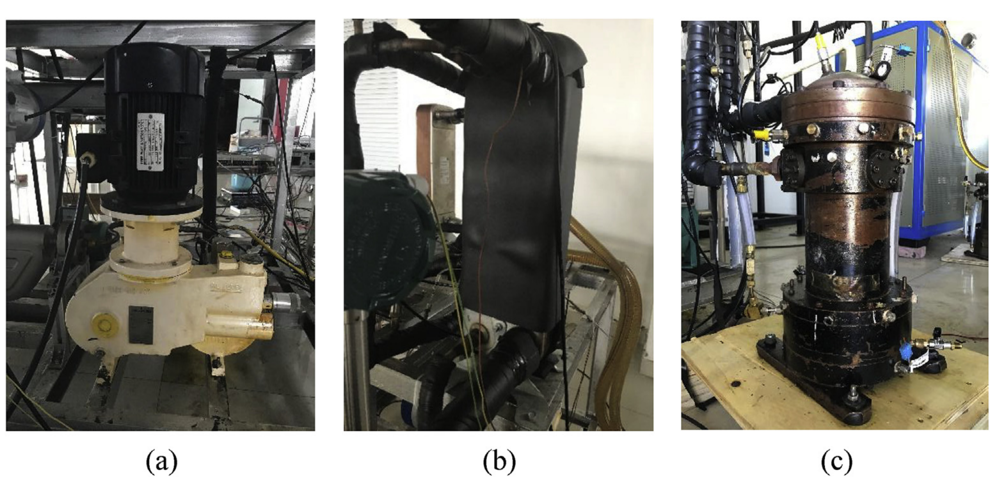

Fig. 7. (a) Liquid pump (b) Plate heat exchanger (c) Hermetic scroll expander.

stable operation of the system. The liquid tank is used to ensure the subcooling status of working fluid at the inlet of the feed pump to avoid the cavitation corrosion. Two cut-off valves are added in the test rig. One is placed at the inlet of the expander and another by-pass valve is equipped for the emergency shut down to ensure the operation safety of system. A sight glass is installed at the outlet of the evaporator to confirm that there is no liquid drop entering the expander. Liquid hammer may decrease the expansion performance to some degree. An oil sight glass is utilized to observe the oil cycle inside the hermetic scroll expander. Sufficient lubricant oil is required to ensure the successive operation of the expander. Characteristics of each component used in current test bench are described in Table 5. At each inlet and outlet of configurations, pressure and temperature sensors are installed to measure the operating conditions of working fluid. A Coriolis-type mass flow-meter is placed at the outlet of liquid pump to measure the refrigerant mass flow rate. Table 6 summarizes the measuring range and accuracy of each sensor.

3.2. Measurement equipment (uncertainties & steady state)

Table 6 lists the measurement devices and the accordingly measurement range and the accuracy of sensors. The formula developed by Moffat [19] is applied to conduct the uncertainty analysis of the system. The dependent variable uncertainty is calculated based on Equation (1), where R represents the function of independent variables and w is referred to their uncertainties. According to the method mentioned above, the calculated accuracies of the cycle thermal efficiency, net power output, expander isentropic efficiency are within 1.1%, 0.8%, 1.1%, respectively.

Table 5
Summary of main ORC configuration characteristics.

Pump		
Plunger diagram pump	manufactures	Milton Roy
	Maximum discharge pressure (kPa)	3000
Evaporator/Condenser		
Brazed plate (Single-pass, Counterflow)	Plate Material	Alumina
	Number of plates	19
Expander		
Hermetic scroll compressor (run in reverse as an expander)	Shell material	ASTM A1020
	Maximum speed (RPM)	3600
	Displacement (compressor mode) (cc)	50
	Built-in volume ratio	2.2
	Displacement (Expander mode) (cc)	22.72
Cut-off valve	Material	Copper
Sight glass	Material	Copper

Table 6
Accuracy of measurement devices.

Measurement	Type	Range	Accuracy
Temperature	RTD 100	−200 °C-+300 °C	±0.5%
Pressure Abs	Electronic pressure transducer (gauge)	0–1000 kPa	±0.5%
Mass flow rate (working fluid)	Coriolis effect	0–600 kg/h	±0.5%
Volume flow rate (Cold water)	LWGY-10BIC1	1–10 m^3/h	±0.5%
Power monitor	DU4-W	0–2500 W	±0.3%

$$W_R = \left(\left(\frac{\partial R}{\partial X_1}w_1\right)^2 + \left(\frac{\partial R}{\partial X_2}w_2\right)^2 + \ldots + \left(\frac{\partial R}{\partial X_n}w_n\right)^2\right)^{1/2} \quad (1)$$

A digital multi-meter along with an armature relay multiplexer are used to record the measured data from devices. The fluctuation range of the measured parameters was used to determine the steady-state, where the fluctuation range is lower than 1% on each variable. During the measurement period of 10 min, all measured values are logged every second.

3.3. Experimental methodology

The prototype of organic Rankine cycle test rig was designed for R245fa, which has been optimized as a baseline beforehand. The current study was targeted to experimentally investigated the applicability of three low-GWP refrigerants including R1233zd(E), R1234ze(Z) and R1336mzz(E) as drop-in replacements to R245fa in the test bench. Furthermore, to analyze the impact of the processing parameters including mass flow rate and the expander rotational speed on the system performance, the optimal operating conditions of R245fa was chosen as the reference set under a given heat source temperature.

Table 7 describes the boundary conditions of the test bench. The heat source temperature is 125 °C with volume flow rate around 4 m^3/h and the cooling water is 28 °C in summer condition with volume flow rate around 9 m^3/h. Control options are assigned to the refrigerant mass flow rate and the expander rotational speed. First of all, a reference parameter set is defined according to the previous baseline tests of R245fa (e.g. Mass flow rate is 205 kg/h and expander rotational speed is 1800 rpm). Starting from the aforementioned reference parameter set, one of the operational parameters (mass-flow rate or expander rotational speed) is varied while another is kept constantly. The selected reference parameter set along with the operating points are all summarized in Table 8. In the first experiment series, the expander rotational speed is maintained at 1800 rpm while the mass flow rate is adjusted to different values within a range between 100 and 300 kg/h. In the second experiment series, the mass flow rate is maintained at 205 kg/h while the expander rotational speed is adjusted to different values within a range between 1400 and 3000 rpm. The spread of performance indicators will be formed according to the variable operational parameters in the lateral section.

4. Results and discussion

This section starts with the analysis of three main components including the scroll expander, the evaporator and the liquid pump. Simultaneous investigation of expansion behavior and heat transfer

Table 7
Boundary conditions.

Loop	Inlet temperature [°C]	Flow rate [m^3/h]
Heating loop	125	4
Cooling loop	28	9

Table 8
Summary of operating conditions.

Operational parameter	Reference parameter set	Variation of $\dot{M}$	Variation of RPM
$\dot{M}$ [kg/h]	205	100–300	205
RPM	1800	1800	1400–3000

procedure are conducted. Pump energy consumption of four refrigerants is also analyzed. Additionally, a comparative analysis of the cycle performance of ORC using four different refrigerants is implemented.

4.1. Expander performance

Expander isentropic effectiveness along with the filling factor are presented as two main dimensionless expander efficiencies, which give an important insight into the expander behavior. The filling factor in Equation (2) is commonly used to qualify the volumetric performance of the scroll expander [20–22].

$$\varphi = \frac{\dot{M}_r v_{in}}{N_{rot} V_{s,x}} = \frac{\dot{M}_r v_{in}}{N_{rot} V_{s,cp}/r_v} \tag{2}$$

where $\dot{M}_r$ is referred to the refrigerant mass flow rate; $V_{s,cp}$ and $V_{s,x}$ are presented as the swept volume of scroll machine in compressor and expander mode, respectively; r_v represents the built-in volume ratio and v_{in} is the suction specific volume flow rate of the expander. Lastly, N_{rot} is referred to the expander rotational speed.

In Fig. 8, the mass flow rate is kept constant around 205 kg/h and the spread of the filling factor is due to different expander rotational speeds. Filling factor is defined as the ratio of the practical volume flow rate and the ideal one. The filling factor greater than a unit indicates the internal leakage occurs inside the scroll expander. Existence of the internal leakage may decrease the expansion performance drastically and therefore affects the system performance. In Fig. 8a, the filling factors of four refrigerants decrease with higher expander rotational speed, which indicates that increasing expander rotational speed enables to reduce the internal leakage. The internal leakage inside the scroll expander is related to the revolution time and leakage path. Longer time results into more internal leakage. Higher expander rotational speed indicates time for per revolution is smaller, thus, the leakage is smaller.

Apart from the impact of the rotary speed, for a certain expander, different refrigerants thermodynamic properties also influence the filling factor. As can be seen in Fig. 8a, R1233zd(E) and R1234ze(Z) show very similar performance in filling factor, both of them indicate more internal leakage than R245fa, which can be explained by the lower fluid density at the expander suction port. For a given mass flow rate, lower fluid density results in larger inlet volume flow rate. When the ideal inflow volume rate is fixed, the filling factor will increase, as can be seen in Equation (2). Comparing the filling factor, R1336mzz(E) showed the most similar behavior to R245fa in current used hermetic scroll expander.

Another important factor that influences the filling factor is the compatibility between the lubricant oil and refrigerants. The better intersolubility contributes to more oil quantity in the working fluid. The oil density is much higher than the vapor, in that case, the mass quality of the vapor is larger if supply volume flow rate is kept the same. The better compatibility between the lubricant oil and the refrigerant is beneficial for the sealing problem inside the scroll expander. Thus, the possibility of the internal leakage is smaller. Selection of appropriate lubricant for a certain working fluid is necessary to improve the expander performance.

Equation (3) describes the definition of the expander isentropic effectiveness. It is defined as the ratio of the output electrical power to the theoretical expansion power.

$$\varepsilon_{is} = \frac{P_e}{\dot{M}_r (h_{su,x} - h_{ex,is,x})} \tag{3}$$

where P_e represents the output electrical power; $h_{su,x}$ and $h_{ex,is,x}$ are referred to the supply specific enthalpy and isentropic exhaust specific enthalpy of the scroll expander, respectively. Fig. 8b depicts the evolution of expander isentropic effectiveness to the operating pressure ratio. The operating pressure ratio is defined as the ratio of the expander inlet pressure to that at the expander outlet. As what is mentioned before, the built-in volume ratio is considered as one of important design parameters of expansion machine. The designed value of the hermetic scroll expander utilized in current study is 2.2. The deviation between the operating pressure ratio and the designed one may bring the under/over expansion loss, which subsequently decreases the expansion performance. In Fig. 8b, firstly the expander isentropic efficiency increases with the pressure ratio and the then decreases for all of the refrigerants. Obviously, the peak of the expander isentropic effectiveness occurs at different operating pressure ratio. For R245fa, R1233zd(E) and R1234ze(Z), the range of operating pressure ratio is between 2.3 and 3.8. The peak of the efficiency occurs at a pressure ratio larger than 2.2. This is mainly because of the internal leakage and mechanical friction loss, which contributes to the higher optimal pressure ratio than the designed one. Generally, higher pressure ratio is beneficial for more output electricity. However, the pressure ratio of R1336mzz(E) is limited to 1.6–2.8. It was assumed that

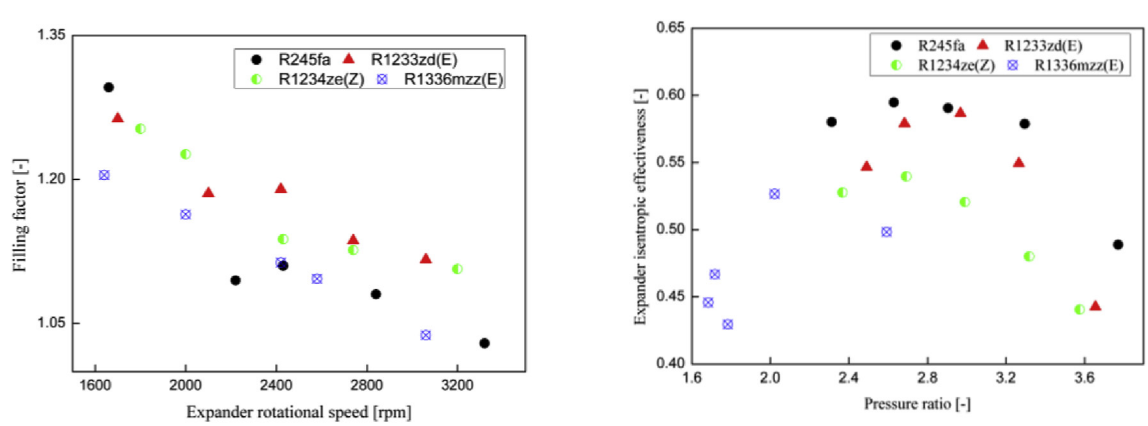

(a) (b)

Fig. 8. (a) Evolution of filling factor to expander rotational speed (b) Evolution of expander isentropic efficiency to pressure ratio.

most of the working points of R1336mzz(E) were located at an under-expansion situation. In that case, the output electricity was much smaller than that of another three refrigerants, thus, the extremely low expander isentropic effectiveness of R1336mzz(E) can be explained. The maximum expander isentropic effectiveness of R245fa is 59.5% while for R1233zd(E), it is 58.5% and 54% for R1234ze(Z). Less internal leakage and high pressure ratio contribute to the slightly higher expander efficiency of R245fa than another two alternatives for current operating conditions.

4.2. Heat exchanger performance

This section presents a comparative analysis among four refrigerants in heat transfer procedure in evaporator. The expander rotational speed was fixed at 1800 rpm constantly while the mass flow rates were adjusted to various values within a range between 100 and 300 kg/h. Regarding of the heat transfer performance, two main factors are involved including the heat transfer coefficient and the pressure drop. On account of that, a dimensionless performance indicator developed by Wang CC [23] was introduced in this section, as shown in Equation (4). The main advantages of such dimensionless indicator have twofold: 1) first is to give an overall evaluation of the new substitute performance in a certain heat exchanger compared to the reference; 2) second is to compare the heat transfer performance of the modified heat exchanger to the baseline one for a specific refrigerant of interest.

$$\xi = \frac{\frac{j}{j_{ref}}}{\left(\frac{f}{f_{ref}}\right)^{1/3}} \tag{4}$$

The objective equation mentioned above is designed for a comprehensive comparison between the alternatives and the reference refrigerant (e.g. R245fa in current study) in a certain evaporator. Here j represents the Colburn factor, which is highly related to heat transfer procedure; f is referred to the Fanning friction number, which is involved with the pressure drop. Equations (5) and (6) are mentioned as empirical formulas for plate type heat exchanger developed by Chisholm and Wanniarchici (1991); β is referred to the chevron angle (e.g. 60°in this research) and formulas are fit for 3000 < Re < 10ˆ5.

$$j = 0.72\cdot\left(\frac{\beta}{30}\right)^{0.66}\cdot Re^{0.59} \tag{5}$$

$$f = 0.8\cdot\left(\frac{\beta}{30}\right)^{3.6}\cdot Re^{-0.25} \tag{6}$$

Lumped parameter method (LPM) was applied to calculate the refrigerant thermodynamic properties. Average values of j and f were obtained for all of the working fluids. Fig. 9 provides a comparison among the evolution of dimensionless indicator of four refrigerants varied with different mass flow rates. For current used brazed plate type evaporator, increasing mass flow rate is beneficial to improve the heat transfer performance since the heat transfer procedure is significantly enhanced with higher working fluid velocity.

The results showed that R1234ze(Z) has similar performance in evaporator to R245fa. Moreover, both of them indicated better heat transfer performance than that of R1233zd(E) and R1336mzz(Z). This is mainly because of larger Reynold number under the same operating condition. On account of this, R1234ze(Z) was considered as the most appropriate drop-in replacement to R245fa.

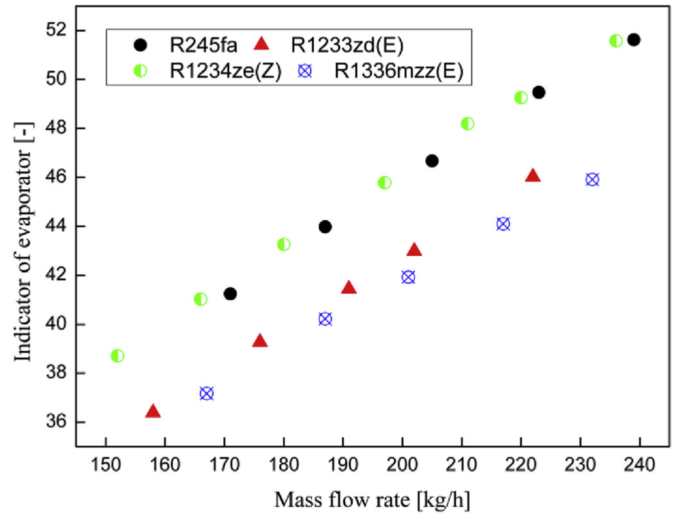

Fig. 9. Comparison of heat exchanger performance indicator.

4.3. Pump performance

Apart from the expansion behavior and heat transfer procedure in evaporator, pump energy consumption is also one of important constituent parts of cycle thermal efficiency. This section aims to present a comparative analysis of pump work among four refrigerants.

In the first analysis, the mass flow rate is maintained at 205 kg/h while the expander rotational speed is varied to different values. Fig. 10a shows the spreads of pump work to various expander rotational speeds of four refrigerants. It shows that pump work decreases with the increasing expander rotational speed. This is mainly because the evaporating pressure of the system decreases with the higher expander rotational speed. In that case, a trade-off balance between aforementioned twofold is demanded to ensure the optimal operating performance of system for a given operating condition.

In the second analysis, the expander rotational speed is fixed at 1800 rpm while the mass flow rate is varied to different values. The evolution of pump work in Fig. 10 b can be understood in the same manner as Fig. 10a. The increasing mass flow rate contributes to the higher outlet pressure of the liquid pump, which results in the increased pump energy consumption.

Comparing the pump energy consumption among different working fluids, R245fa, R1233zd(E) and R1234ze(Z) resemble to each other in two experimental series while R1336mzz(E) consumes the least pump work. From the systematic point of view, pump performance is influenced by the expansion behavior on expander side. The extremely low operating pressure ratio of R1336mzz(E) results in the under-expansion loss, which brings down the expansion performance. The pressure drop was relatively lower than another three refrigerants, in turn, the pump energy consumption is smaller.

4.4. Cycle performance

Cycle performance is a comprehensive result with understanding the behavior of individual components. In this section, systematic performance of organic Rankine cycle using four different refrigerants is compared. Boundary conditions have been provided in Table 7. Mass flow rates and expander rotational speed are two degree of freedoms of ORC system. Considering the large number of working points, one mutual operating condition (e.g. 205 kg/h,

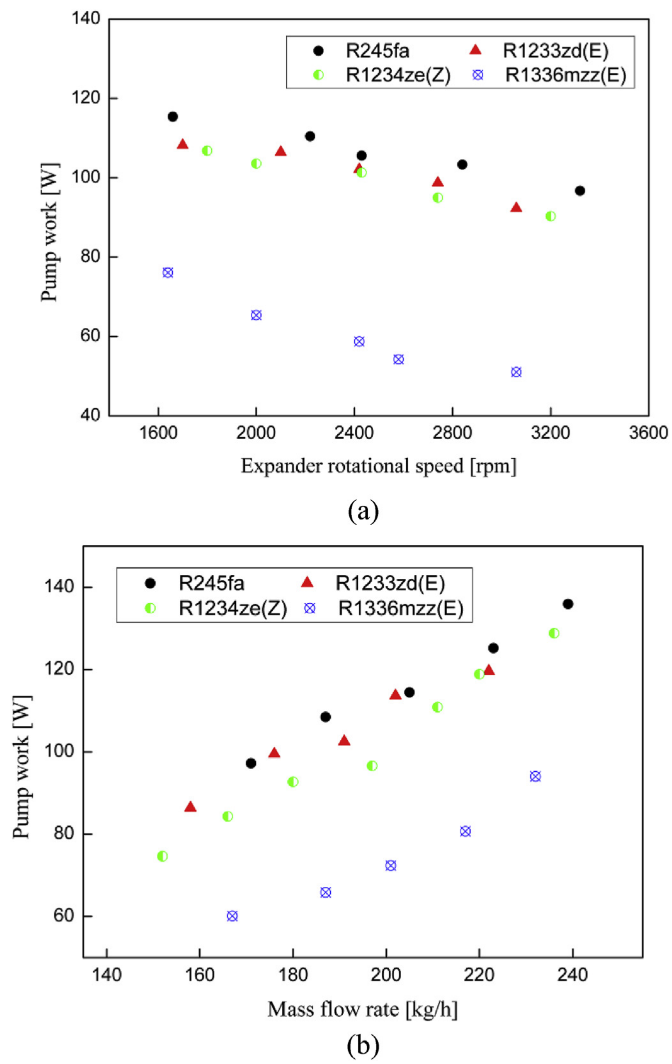

Fig. 10. (a) Evolution of pump work to expander rotational speed (b) Evolution of pump work to mass flow rate.

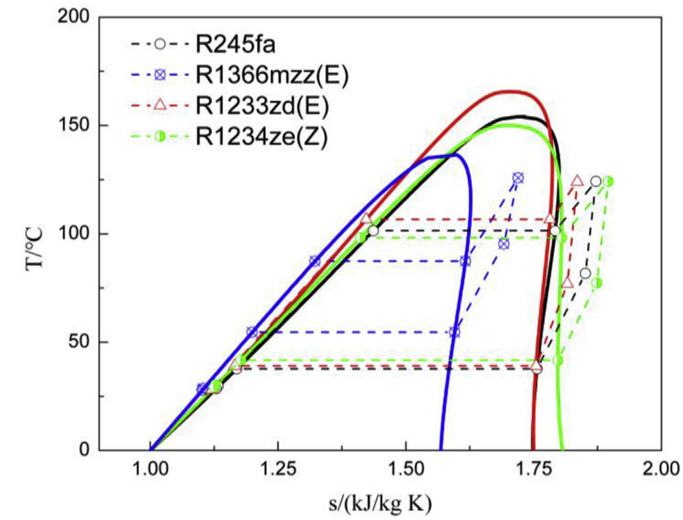

Fig. 11. Operating process in T-*s* diagram.

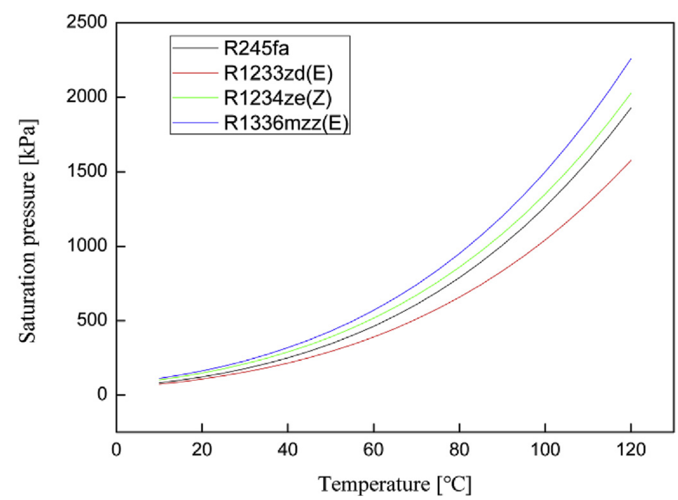

Fig. 12. Evolution of saturation pressure to temperature of four refrigerants.

2400 rpm) is chosen to distinguish the differences in cycle performance among four working fluids. The operating temperatures of four refrigerants are listed in Table 9. In Fig. 11, R1233zd(E) and R1234ze(Z) indicate very similar performance to R245fa while R1336mzz(E) shows the relatively lower evaporating temperature, which is mainly because of the lower saturation temperature, as can be seen in Fig. 12. In addition, the condensing temperature of R1336mzz(E) is higher than the rest of refrigerants. Thermodynamic analysis has proved that higher saturation temperature is beneficial to improve the cycle thermal efficiency while higher condensing temperature may decrease cycle performance. This is because for the same operating pressure, higher evaporating temperature can be achieved by refrigerant with higher saturation temperature. The deviation between the evaporating and condensing pressures decides the potential expansion work on expander side. In a word, the evolution trends in experimental tests are consistent with theoretical thermodynamic analysis.

Further analysis of whole operating condition is also implemented in this section. System performance can be evaluated with the cycle thermal efficiency and the net power output. In Figs. 13–14, two types of operating conditions are depicted. Fig. 13a showed the evolution of net power output to the increasing mass flow rate under a fixed expander rotational speed of 1800 rpm. It's well known that higher mass flow rate contributes to lager output electricity. R1234ze(Z) and R1233zd(E) shows very similar performance to R245fa while R1336mzz(Z) leads to the lowest net power output. This is mainly because of the limitation of the extremely smaller operating pressure ratio and relatively higher condensing temperature of R1336mzz(E) compared to the rest of refrigerants.

Table 9
Operating temperature of four refrigerants.

Parameters	R245fa	R1233zd(E)	R1234ze(Z)	R1336mzz(E)
Evaporating temperature [°C]	101.4	106.7	98.2	87.4
Condensing temperature [°C]	37.7	39.0	41.6	54.5

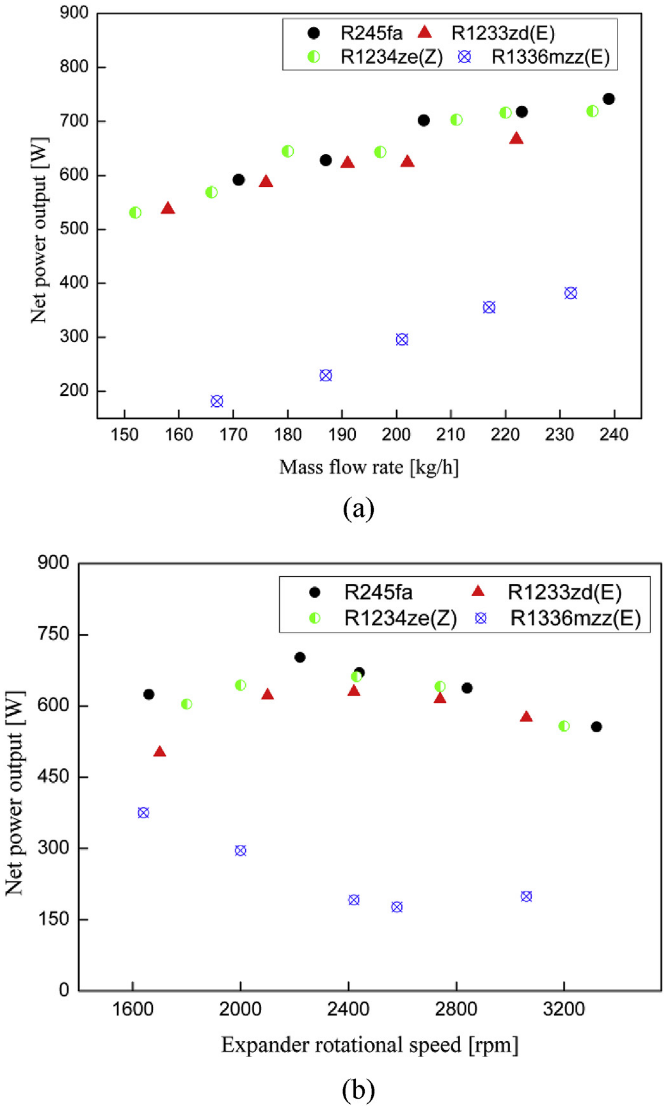

Fig. 13. (a) Evolution of net power output to mass flow rate (b) Evolution of net power output to expander rotational speed.

Fig. 13b presents the evolution of net power output to the expander rotational speed. Considering the internal leakage under the lower expander rotational speed and increasing friction loss under higher rotate speed, the net power electricity increases firstly and then decreases for R245fa, R1233zd(E) and R1234ze(Z). However, for R1336mzz(E), the evolution trend is completely different. The net power output decreased drastically as the expander rotational speed increased. This is because the most of the operating pressure ratios are located in the under-expansion region, the peak of net power output occurs at the beginning of the curve and the evolution trend is monotonic. Fig. 14 describes the evolution of cycle thermal efficiency to the operational parameters. In Fig. 14a, the maximum cycle thermal efficiency is obtained by R1233zd(E) around 4.7%. In Fig. 14b, R1234ze(Z) almost had the same cycle thermal efficiency to R245fa at each working point. Obviously, R1336mzz(E) showed the exactly opposite evolution trends compared to the rest three refrigerants. The reasons have already been presented in previous analysis. It can be concluded that R1336mzz(E) is not suitable as drop-in replacement to R245fa for current operating conditions. More different heat source temperatures should be investigated in the future by researchers.

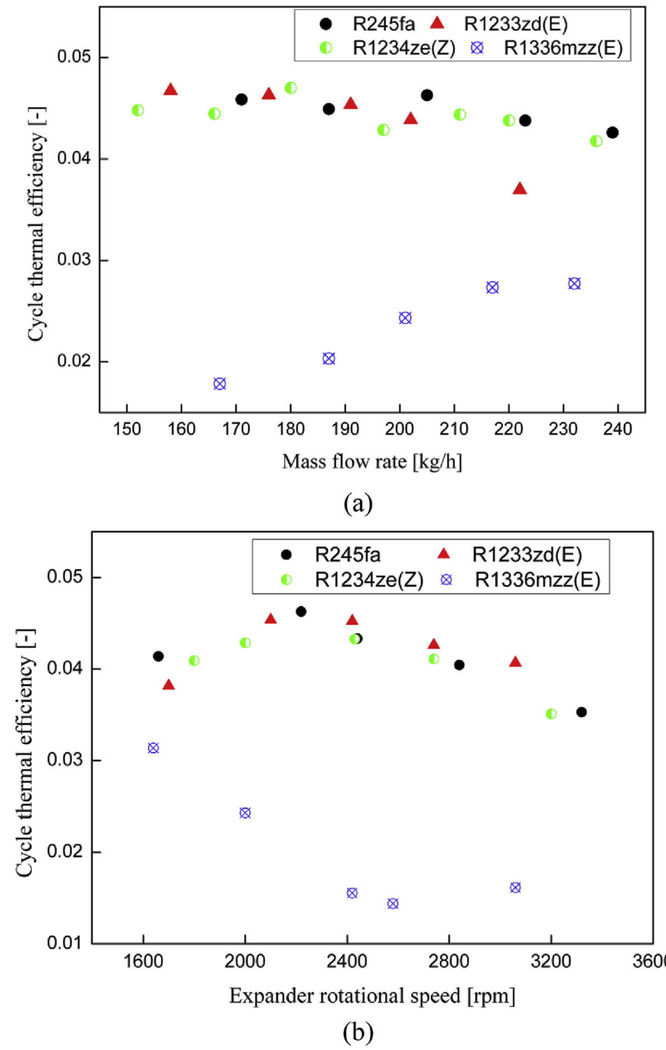

Fig. 14. (a) Evolution of cycle thermal efficiency to mass flow rate (b) Evolution of cycle thermal efficiency to expander rotational speed.

Compared to the ideal thermodynamic analysis without consideration of pressure drop and heat transfer loss, the practical experimental tests can be quite different since nonlinear behavior of each individual configuration. Tiny difference in thermodynamic properties of refrigerants may result in distinct behavior in systematic performance. In order to better take advantage of new low-GWP refrigerants, further optimization of components based on a mathematical simulation is demanded. Considering the main scope of current study, the numerical investigation and geometric optimization of ORC system will be the next step of authors' research.

5. Conclusions

This paper experimentally investigated three low-GWP refrigerants including R1234ze(Z), R1233zd(E) and R1336mzz(E) as drop-in replacements to R245fa for micro-scale organic Rankine cycle application. The impacts of procession parameters such as refrigerant mass flow rate and expander rotational speed on the cycle thermal efficiency, net power output was analyzed. Additionally, the differences in expansion procedure, heat transfer process in evaporator and pump consumption were compared simultaneously. Several conclusions can be drawn as follows:

1) R1234ze(Z) and R1233zd(E) were proved to be appropriate drop-in replacements to R245fa in current test bench. Similar cycle performance and environmental-friendly properties of both refrigerants show the privilege to R245fa;
2) For the whole range of operating conditions, comparing the maximum cycle thermal efficiency, R245fa is 4.6% while R1233zd(E), R1234ze(Z) and R1336mzz(E) are 4.7%, 4.5% and 3.1%, respectively; Comparing the maximum net power output, R245fa generates 11.4% more than R1233zd(E) and 3.1% than R1234ze(Z).
3) Higher pressure ratio contributes to larger output electrical power. The extremely lower efficiency of R1336mzz(E) is limited by the smaller pressure ratio range. Internal leakage inside the scroll expander can be improved by increasing expander rotational speed. Apart from that, the compatibility between the lubricant oil and refrigerants also has great impact to the sealing performance. In that case, selection of appropriate lubricant oil for a certain working fluid is necessary.
4) In terms of the heat transfer performance inside the plate type heat exchanger, R1234ze(Z) exhibits the most similar behavior to R245fa. Both of them lead to better heat transfer performance than R1233zd(E) and R1336mzz(E).

Acknowledgement

This work was supported by Shanghai high efficient cooling system Research Center.

Nomenclature

h	Specific enthalpy [kJ/kg]
$\dot{M}$	Mass flow rate [kg/h]
N	Expander rotational speed [rpm]
P	Electrical power [W]
$\dot{Q}$	Heat rate [W]
rv	Built-in volume ratio [-]
v	Specific volume flow rate [m^3/kg]
$\dot{W}$	Power work [W]

Greek

ε	Expander isentropic efficiency [-]

Acronyms

CHP	Combined heat and power
EOS	Equation of state
GHG	Green-house gas
GWP	Global Warming Potential
HFO	Hydrofluoroolefins
ODP	Ozone Depletion Potential
ORC	Organic Rankine cycle

Subscripts

cp	compressor
e	electrical
x	expander
ev	evaporator
is	isentropic
in	inlet
p	pump
ref	refrigerant
rot	rotational
su	supply
s	swept

References

[1] United Nations, Kyoto protocol to the united nations framework convention on climate change.
[2] The European Parliament and the Council of the European Union, Directive 2006/40/ec of the European parliament and the council of the European Union of 17 may 2006 relating to emissions from air-conditioning systems in motor vehicles and amending council directive 70/156/eec.
[3] http://conf.montreal-protocol.org/meeting/mop/mop-28/final_report/English/MOP28-Dec1.docx (Ozone Sec Secretariat Conference Portal).
[4] Yamada N, Mohamad MNA, Kien TT. Study on thermal efficiency of low- to medium-temperature organic Rankine cycles using HFO-1234yf. Renew Energy 2012;41:368–75.
[5] Luo D, Mahmoud A, Cogswell F. Evaluation of low-GWP fluids for power generation with organic rankine cycle. Energy 2015;85:481–8.
[6] Liu W, Meinel D, Wieland C, Spliethoff H. Investigation of hydrofluoroolefins as potential working fluids in organic Rankine cycle for geothermal power generation. Energy 2014;67:106–16.
[7] Petr P, Raabe G. Evaluation of R-1234ze(Z) as drop-in replacement for R-245fa in Organic Rankine Cycles - from thermophysical properties to cycle performance. Energy 2015;93:266–74.
[8] Ziviania Davide, Dickes Rémi, Quoilin Sylvain, Lemort Vincent, De Paepe Michel, van den Broek Martijn. Organic Rankine cycle modelling and the ORCmKit library: analysis of R1234ze(Z) as drop- in replacement of R245fa for low-grade waste heat recovery. In: The 29th international conference on efficiency, cost, optimization, simulation and environmental impact of energy systems; 2016. p. 1–13.
[9] Usman M, Imran M, Yang Y, Lee DH, Park B-S. Thermo-economic comparison of air-cooled and cooling tower based Organic Rankine Cycle (ORC) with R245fa and R1233zde as candidate working fluids for different geographical climate conditions. Energy 2017;123:353–66.
[10] Moles F, Navarro-Esbrí J, Peris B, Mota-Babiloni A, Barragan-Cervera Á, Kontomaris K. Low GWP alternatives to HFC-245fa in Organic Rankine Cycles for low temperature heat recovery: HCFO-1233zd-E and HFO-1336mzz-Z. Appl Therm Eng 2014;71(1):204–12.
[11] Nagata R, Kondou C, Koyama S. Comparative assessment of condensation and pool boiling heat transfer on horizontal plain single tubes for R1234ze(E), R1234ze(Z), and R1233zd(E). Int J Refrig 2016;63:157–70.
[12] Navarro-Esbrí J, Moles F, Peris B, Mota-Babiloni A, Kontomaris K. Experimental study of an Organic Rankine Cycle with HFO-1336mzz-Z as a low global warming potential working fluid for micro-scale low temperature applications. Energy 2017;133:79–89.
[13] Guillaume L, Legros A, Desideri A, Lemort V. Performance of a radial-inflow turbine integrated in an ORC system and designed for a WHR on truck application: an experimental comparison between R245fa and R1233zd. Appl Energy 2017;186:408–22.
[14] Eyerer S, Wieland C, Vandersickel A, Spliethoff H. Experimental study of an ORC (Organic Rankine Cycle) and analysis of R1233zd-E as a drop-in replacement for R245fa for low temperature heat utilization. Energy 2016;103:660–71.
[15] https://eur-lex.europa.eu/legal-content/EN/TXT/?uri=uriserv:OJ.L_.2014.150.01.0195.01.ENG.
[16] E.W. L, M.L. H, M.O. M, editors. NIST standard reference Database 23: reference fluid thermodynamic and transport properties-REFPROP. Version 9.1. Gaithersburg: National Institute of Standards and Technology; 2013.
[17] Song P, Wei M, Shi L, Danish SN, Ma C. A review of scroll expanders for organic Rankine cycle systems. Appl Therm Eng 2015;75:54–64.
[18] Zywica G, Kaczmarczyk TZ, Ihnatowicz E. A review of expanders for power generation in small-scale organic Rankine cycle systems: performance and operational aspects. J Power and Energy 2016;230(7):669–84.
[19] Moffat RJ. Describing the uncertainties in experimental results. Exp Therm Fluid Sci 1998;1:3–17.
[20] Laboratories W Herrick, Woodland Brandon J, Braun James E, Horton W Travis. Experimental testing of an organic rankine cycle with scroll-type expander. Publications of the Ray W. Herrick Laboratories. Paper 52.
[21] Enrico Bocci, Maurizio Cambi, Andri. Converting a commercial scroll compressor into an expander: experimental and analytical performance evaluation. Energy Procedia 2017;129:363–70.
[22] Lemort V, Declaye S, Quoilin S, Experimental characterization of a hermetic scroll expander for use in a micro-scale Rankine cycle. Proc IME J Power Energy. Vol. 226.
[23] Chi-Chuan Wang, Heat exchangers-thermal design. 978-957-11-4764-2, 900.